

## Testing epitaxial $\text{Co}_{1.5}\text{Fe}_{1.5}\text{Ge}(001)$ electrodes in MgO-based magnetic tunnel junctions

A. Neggache,<sup>1,2</sup> T. Hauet,<sup>1</sup> F. Bertran,<sup>2</sup> P. Le Fèvre,<sup>2</sup> S. Petit-Watelot,<sup>1</sup> T. Devolder,<sup>3</sup> P. Ohresser,<sup>2</sup> P. Boulet,<sup>1</sup> C. Mewes,<sup>4</sup> S. Maat,<sup>5</sup> J. R. Childress,<sup>5</sup> and S. Andrieu<sup>1,a)</sup>

<sup>1</sup>Institut Jean Lamour, UMR CNRS 7198, Université de Lorraine, 54506 Vandoeuvre lès Nancy, France

<sup>2</sup>Synchrotron SOLEIL-CNRS, L'Orme des Merisiers, Saint-Aubin BP48, 91192 Gif-sur-Yvette, France

<sup>3</sup>Institut d'Electronique Fondamentale, CNRS, UMR 8622, 91405 Orsay, France

<sup>4</sup>Department of Physics and Astronomy/Center for Materials for Information Technology, University of Alabama, Tuscaloosa, Alabama 35487, USA

<sup>5</sup>San Jose Research Center, HGST, a Western Digital company, San Jose, California 95135, USA

(Received 24 May 2014; accepted 13 June 2014; published online 26 June 2014)

The ability of the full Heusler alloy  $\text{Co}_{1.5}\text{Fe}_{1.5}\text{Ge}(001)$  (CFG) to be a Half-Metallic Magnetic (HMM) material is investigated. Epitaxial CFG(001) layers were grown by molecular beam epitaxy. The results obtained using electron diffraction, X-ray diffraction, and X-ray magnetic circular dichroism are consistent with the full Heusler structure. The pseudo-gap in the minority spin density of state typical in HMM is examined using spin-resolved photoemission. Interestingly, the spin polarization found to be negative at  $E_F$  in equimolar CoFe(001) is observed to shift to positive values when inserting Ge in CoFe. However, no pseudo-gap is found at the Fermi level, even if moderate magnetization and low Gilbert damping are observed as expected in HMM materials. Magneto-transport properties in MgO-based magnetic tunnel junctions using CFG electrodes are investigated via spin and symmetry resolved photoemission.

© 2014 AIP Publishing LLC. [<http://dx.doi.org/10.1063/1.4885354>]

The material science community is putting a large effort into developing original magnetic materials for the implementation in low-energy spintronic devices. An important part of this work is devoted to growing electrode materials for Magnetic Tunnel Junctions (MTJs) for Magnetic Random Access Memory (MRAM), oscillators, and sensors. Thin magnetic electrodes having high spin-polarization, low damping, moderate magnetization, and high perpendicular magnetic anisotropy are investigated. The family of Half-Metallic Magnetic (HMM) compounds fulfill these requirements as *ab initio* calculations performed on many Heusler or Half-Heusler compounds (NiMnSb,  $\text{Co}_2\text{FeSi}$ ,  $\text{Co}_2\text{MnSi}$ ...) have predicted a 100% spin polarization at the Fermi energy (leading to infinite tunnel magneto-resistance in theory), extremely low Gilbert damping, high Curie Temperature, and moderate magnetization.<sup>1</sup> Moreover, perpendicular anisotropy has been experimentally achieved for some Heusler alloys.<sup>2</sup>

Recent work performing FerroMagnetic Resonance (FMR) and Giant Magneto-Resistance (GMR) measurements tend to show that  $\text{Co}_{1.5}\text{Fe}_{1.5}\text{Ge}$  (CFG) compound could be very promising since low damping<sup>3</sup> and high GMR<sup>4</sup> were reported. *Ab initio* calculations of the related full Heusler alloy  $\text{Co}_2\text{FeGe}$  Density Of States (DOS) show that a pseudo-gap exists in the integrated minority spin DOS. Nevertheless, the Fermi level sits in the higher edge of this band gap.<sup>5,6</sup> Takahashi *et al.* substituted Ge by Ga atoms to change the number of valence electrons and, thus, to shift the Fermi level towards the middle of the band gap.<sup>7</sup> Assuming a  $\text{L}_{21}\text{Co}_2\text{FeGa}_x\text{Ge}_{1-x}$  (CFGG) structure, they reported up to 70%

spin-polarization measured with point contact Andreev reflection as well as more than 40% GMR at room temperature in CFGG/Ag/CFGG metallic spin-valves. In parallel, *ab initio* calculations<sup>3</sup> show that substituting Co by Fe atoms—thus maintaining a B2 ordered phase—will shift the Fermi level into the minority band gap. In addition, increasing the Fe relative to the Co concentration favors optimized chemical ordering since Co atoms in Fe or Ge sites destroy the pseudo-gap, although Fe atoms in Ge sites keep it unaffected. Calculations seem to be confirmed by the spin-wave Doppler technique which was used to measure the spin-drift velocity of the magnetization in current-carrying CFG and yielded an up to 95% current polarization for CFG.<sup>8</sup> Finally, the Curie temperature of  $\text{Co}_2\text{FeGe}$  has been measured close to 1000 K,<sup>6</sup> and perpendicular anisotropy for iron rich  $\text{Co}_{20}\text{Fe}_{50}\text{Ge}_{30}$  has been demonstrated when sandwiched between MgO layers,<sup>2</sup> due to the perpendicular interface anisotropy induced by MgO.<sup>9</sup> Therefore, all these features make CFG a promising candidate for magnetic-RAM electrode. However, CFG has not been successfully integrated in MTJ's so far and its spin-polarization at and below the Fermi level has not yet been measured.

In this Letter, we report on experimental studies of single crystal  $\text{Co}_{1.5}\text{Fe}_{1.5}\text{Ge}(001)$  layers as single films or as electrodes in MgO-based MTJ's. First, the growth and structural characterization of CFG on MgO(001) substrates is discussed. Gilbert damping and magnetic features are extracted from FMR and magnetometry measurements. The spin-polarization of occupied electronic states is determined using spin-resolved photoemission spectroscopy at the SOLEIL synchrotron source. Finally, transport measurements performed on CFG/MgO/CFG(001) and  $\text{Co}_{25}\text{Fe}_{75}/\text{MgO}/\text{CFG}(001)$  MTJs are presented.

<sup>a)</sup>Author to whom correspondence should be addressed. Electronic mail: [stephane.andrieu@univ-lorraine.fr](mailto:stephane.andrieu@univ-lorraine.fr)

Single CFG films were grown by molecular beam epitaxy (base pressure  $10^{-10}$  Torr) on MgO(001) single-crystal substrates. The CFG single layers were grown by co-evaporating Co, Fe, and Ge using 3 Knudsen cells whose fluxes were calibrated by using a quartz microbalance located at the sample position. The uncertainty on the concentrations is estimated to be  $\pm 5\%$ . The films were deposited on MgO at room temperature, and annealing temperatures were tested in the range of  $350^\circ\text{C}$ – $700^\circ\text{C}$ . Three types of MTJs were grown on MgO(001) substrates. Here, we will mostly discuss MTJ's with structure: Fe (20 nm)/CFG (4 nm)/MgO (2.4 nm)/CFG (8 nm)/Co (20 nm)/Au (10 nm) and  $\text{Co}_{25}\text{Fe}_{75}$  (50 nm)/MgO (2.4 nm)/CFG (30 nm)/Co (20 nm)/Au (10 nm). The CFG electrodes were deposited at room temperature and then annealed during 30 min at temperatures between  $350^\circ\text{C}$  and  $500^\circ\text{C}$ . The whole stacking was subsequently patterned by UV-photolithography and a conventional physical etching processes to get MTJ cells with a junction's size of  $10 \times 10$  to  $50 \times 50 \mu\text{m}^2$ .

The structural properties of single CFG films were first analysed during growth using Reflection High Energy Electron Diffraction (RHEED). At room temperature, the RHEED patterns are the same as observed when growing pure Fe films (Fig. 1). The unit cell is, thus, a square of half

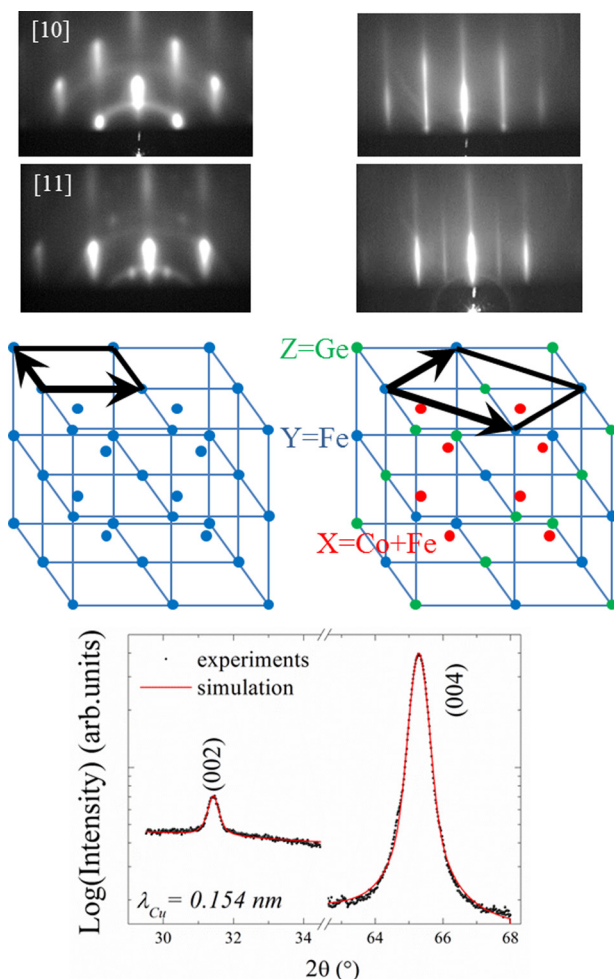


FIG. 1. RHEED patterns obtained on a CFG film as-deposited at RT (top left) and annealed (top right). New  $1/2$  streaks appear after annealing typical of chemical ordering. The (00L) diffraction peak intensities are also well fitted assuming the full Heusler  $\text{L}2_1$  structure (bottom).

the size of the Heusler (001) face, meaning that no chemical ordering occurs. Annealing at  $250^\circ\text{C}$  is sufficient to observe new  $1/2$  streaks appearing along the (11) azimuth of the initial square lattice (Fig. 1), meaning that the lattice cell has doubled in size as expected for the Heusler  $\text{L}2_1$  structure. It should be noted that this superstructure cannot be observed in the case of the full Heusler  $\text{X}_2\text{YZ}$  structure with chemical disorder between Y and Z (B2 phase). In the case of the  $\text{X}_{1.5}\text{Y}_{1.5}\text{Z}$  phase, however, a more complex chemical arrangement cannot be ruled out. This simple observation is a clear indication that some chemical ordering takes place even at low annealing temperatures  $< 300^\circ\text{C}$ .

To go further, X-ray diffraction experiments were performed using a Cu  $\text{K}_{\alpha 1}$  anode ( $\lambda = 0.154 \text{ nm}$ ) along the (001) direction. Fig. 1 shows the typical X-ray  $\theta$ – $2\theta$  diffraction pattern for an annealed CFG film. In addition to the MgO (002) peak (not shown), the pattern shows only the (002) and (004) peaks typical of the Heusler structure. No additional phase (e.g., a parasitic hexagonal phase) has been detected. The lattice spacing is equal to  $0.573 \text{ nm}$  in agreement with values already reported.<sup>4,6,10</sup> The full determination of the species distribution within the lattice is not possible here because the Co and Fe scattering factors are very close using  $\text{K}_{\alpha 1}$  X-rays. However, it is possible to get some information on the location of Ge atoms by fitting the (002) and (004) peaks. A Rietveld refinement was used and an excellent agreement is obtained (simulated curves in Fig. 1) assuming the full Heusler  $\text{L}2_1$  structure. To go further simulations were performed assuming the substitution of some Fe or Co atoms by Ge. We thus were not able to fit the experimental data. However, this simulation does not allow us to eliminate the possibility of some chemical disorder between Fe and Co atoms. Such Co and Fe permutation is predicted to destroy the pseudogap.<sup>3</sup>

The magnetization is also very sensitive to chemical disorder. We performed magnetometry experiments using a commercial VSM with automatic sample rotation. The magnetization at saturation on average is  $1000 \pm 100 \text{ kA/m}$  ( $\text{emu/cm}^3$ ) equivalent to  $5 \pm 0.5 \mu_B$  per unit cell, which is similar to calculated values for  $\text{Co}_2\text{FeGe}$ <sup>6</sup> and experimental values in Ref. 4. A cubic magnetic anisotropy is deduced from the hysteresis loop shape, especially from the value of remanent magnetization as a function of the applied magnetic field angle. X-ray magnetic circular dichroism (XMCD) was also performed on the DEIMOS beamline at SOLEIL (Fig. 2(a)) at the Fe, Co, and Ge 2p edges. A dichroic signal is observed for the 3 elements. The atomic magnetic moments of Fe and Co were found parallel, and antiparallel to the Ge one. The application of the sum rules (using the Fe and Co number of holes in the bulk) gives  $2.0 \pm 0.1 \mu_B/\text{at}$  and  $1.5 \pm 0.1 \mu_B/\text{at}$  for Fe and Co, respectively. The Ge magnetic moment is difficult to determine but is very small (small dichroic signal). Theoretical calculations based on first principles within density-functional theory using the plane-wave ultrasoft pseudo-potential method within the generalized gradient approximation for the exchange-correlation functional<sup>11,12</sup> have been performed to determine the magnetic moments. To study the effect of permutations we have used a 16 atom super cell. The fully relaxed structure has a total magnetic moment of

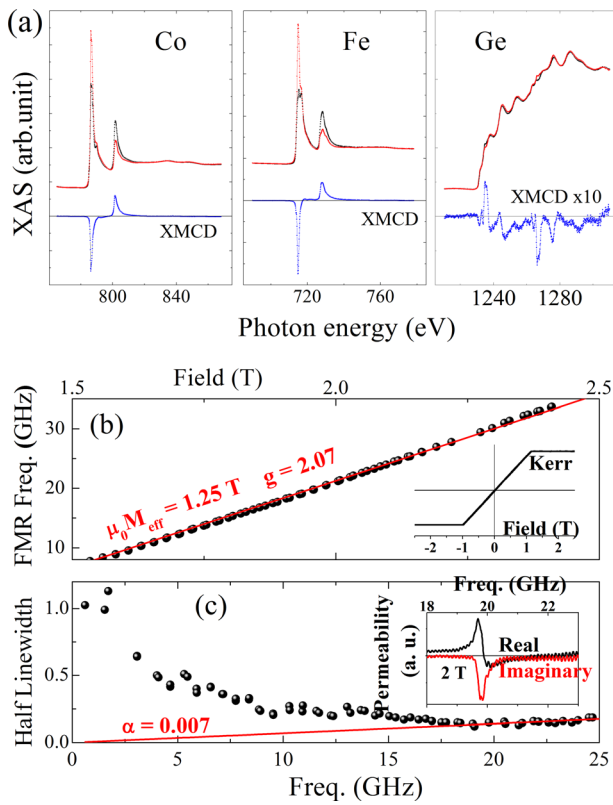


FIG. 2. Magnetic properties of  $(\text{CoFe})_3\text{Ge}$  film using X-Ray absorption spectroscopy (XAS and XMCD) and FMR. (a) The XMCD signal on Ge is opposite to the Fe and Co signals, suggesting that the Ge magnetic moment is coupled antiparallel to Fe and Co. (b) FMR frequency versus perpendicularly applied field. The red line is a linear fit, yielding a Landé factor of 2.07 and a magnetization of 1.25 T. Inset: Polar magneto-optical Kerr effect loop (10 nm film). (c) FMR linewidth versus frequency in perpendicular applied field conditions (30 nm film). Inset: Real and imaginary parts of the permeability for a field of 2 Tesla.

approximately  $5.3 \mu_B$  per unit cell with a Ge magnetic moment equal to  $-0.1 \mu_B/\text{at}$ . Using this value of the Ge moment, we found a magnetic moment for the unit cell of  $(1.5 + 2) \times 1.5 - 0.1 = 5.15 \mu_B$  per unit cell in very good agreement with calculations. Another important theoretical result is that the total magnetic moment decreases to  $4.8 \mu_B/\text{cell}$  when Co atoms take the place of Fe atoms in the FeGe lattice as shown in Fig. 1. Finally, Vector Network Analyzer FerroMagnetic Resonance (VNAFMR see Ref. 13) has been performed at room temperature on a series of CFG samples (Figs. 2(b) and 2(c)). In saturating conditions, the FMR frequency is linear with the perpendicular field and gives an effective magnetization equal to  $1.25 \pm 0.05 \text{ T}$  ( $=995 \pm 40 \text{ kA/m}$  in agreement with SQUID measurements) with a Landé factor equal to  $2.07 \pm 0.02$ . The evolution of the linewidth with the resonance frequency indicates slight contributions of the inhomogeneous broadening, whose influence is gradually suppressed for frequencies up to 17 GHz, above which the subsequent linewidth evolution is consistent with a Gilbert damping  $\alpha$  of  $0.007 \pm 0.001$ . For the 30 nm thick layer, a faint perpendicular standing spin wave mode is detected at 8 GHz above the uniform resonance mode. This splitting is indicative of an exchange stiffness of  $A = 13 \pm 1 \text{ pJ/m}$ .<sup>14</sup> The low damping value is consistent with typical HMM behavior for which the damping coefficient is expected to be very small due to the lack of minority

spin DOS at the Fermi level. All these results are strong indications that chemical disorder is very limited in our films.

The CFG spin polarization was investigated using Spin-Resolved PhotoEmission Spectroscopy (SR-PES) performed on the CASSIOPEE beamline at the SOLEIL synchrotron. Single CFG films were epitaxially grown in a molecular beam epitaxy (MBE) chamber connected to the beamline<sup>15</sup> so that surface contamination is prevented. First SR-PES experiments were conducted with 37 eV  $p$ -polarized light at a  $45^\circ$  incident angle. The photoelectron detection was performed along the (001) normal axis of the films using the largest aperture ( $\pm 8^\circ$ ) leading to investigating 80% of the Brillouin Zone (BZ). The spin resolution was achieved by using a Mott detector. The sample temperature was maintained below 100 K during the experiments. Figures 3(a) and 3(b) show the majority  $N_\uparrow$  and minority  $N_\downarrow$  photoemission spectra (PES) obtained on single CoFe (as reference layer) and single CFG thin films annealed at around  $550^\circ\text{C}$ . The corresponding spin polarizations  $P = (N_\uparrow - N_\downarrow)/(N_\uparrow + N_\downarrow)$  are plotted in Figs. 3(a) and 3(b). In the reference CoFe layer, the expected negative spin polarization is found at  $E_F$  (Fig. 3(a)). The situation is clearly different for CFG films. The main difference between CoFe and CFG consists in a strong majority spin contribution around  $-0.2 \text{ eV}$  leading to a positive polarization peak at the same energy value (Fig. 3(b)). This new majority spin band pushes the spin polarization to become positive close to  $E_F$ . The occurrence of this strong majority spin contribution may be at the origin of the greatly enhanced magnetoresistive properties obtained in CFG spin-valves compared to CoFe.<sup>4</sup> However as might be expected our experiment on CFG spin-valves films shows that the actual spin polarization is  $< 100\%$ .

A final test to evaluate HMM behavior is to use CFG as electrodes in MgO-based MTJs. A first experiment was to grow CFG on Fe/MgO(001) underlayers since the resulting MgO barrier quality is excellent and well understood in this case. The upper electrode was a 10 nm thick CFG layer covered by a thick Co layer resulting in a magnetic coercive

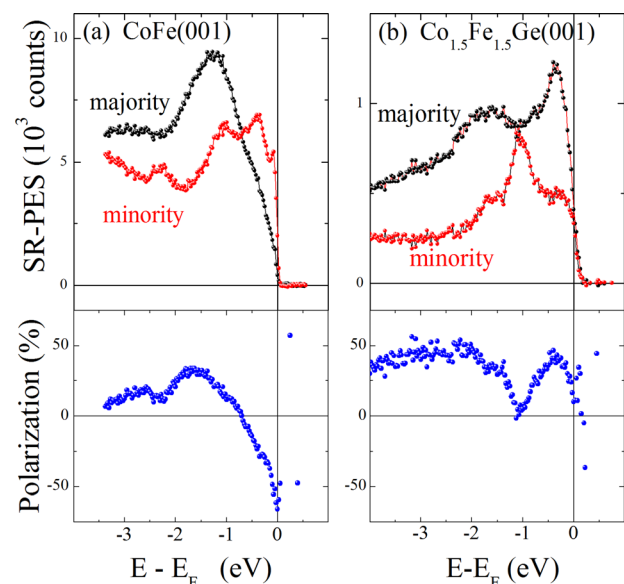


FIG. 3. PES spectra (top) and spin polarization (bottom) for annealed (a) equimolar  $\text{CoFe}(001)$  and (b)  $(\text{CoFe})_3\text{Ge}$  films.



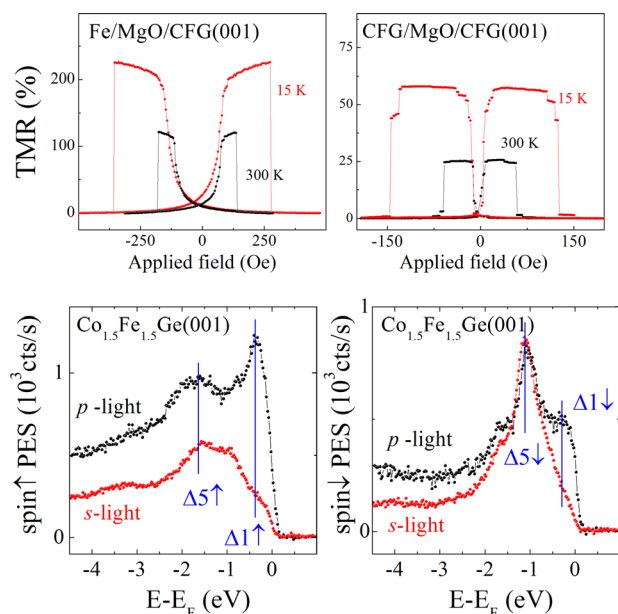


FIG. 4. Top—TMR as a function of magnetic field amplitude measured on a Fe/MgO/CFG(001) MTJ (left) and on a CFG/MgO/CFG(001) MTJ (right). Bottom—SR-PES using *p* and *s* polarization of the photon.  $\Delta_1$  symmetry states are excited using *p*-light but not with *s*-light.  $\Delta_5$  symmetry states are excited using both light polarizations.<sup>15,17</sup> The detection of  $\Delta_1\downarrow$  states at  $E_F$  explains the limited TMR values using CFG electrodes.

field for the upper electrode substantially higher than that of the lower Fe electrode. The CFG layer was grown at RT and annealed up to 550 °C. The Co layer was grown on top of CFG at RT to avoid intermixing. The Tunnel Magneto-Resistance (TMR) vs. *H* curves are shown in Fig. 4. The TMR reaches 125% at RT and more than 220% at 15 K consistent with a good epitaxial process and high spin polarization in the tunneling process. However, these values are smaller than state of the art TMR values obtained on Fe/MgO/Fe(001) (around 200% at RT and 450% at 10 K, see Ref. 16). The TMR is even lower using two CFG electrodes (Fig. 4), where the TMR is only around 15% at RT and 60% at 15 K. To better understand these magneto-transport results, we carefully studied the symmetry of the electronic states near  $E_F$ . The high TMR values in Fe/MgO/Fe system are actually due to the lack of  $\Delta_1$  minority spin DOS at  $E_F$ . We thus performed the SRPES measurement with *s*-polarized light (Fig. 4) in order to identify the symmetry of the observed transitions ( $\Delta_1$  or  $\Delta_5$  see Refs. 15 and 17). We found that the majority spin peak around  $-0.2$  eV has a  $\Delta_1$  symmetry since its contribution using *p*-polarized light is strongly reduced when measuring with *s*-polarized light. But more interestingly, we also observe some  $\Delta_1$  contribution in the minority spin DOS. Such minority spin channel with a  $\Delta_1$  symmetry lowers the overall spin polarization and is detrimental to TMR, which explains the low TMR values obtained using CFG in our MgO-based MTJs.

To summarize, single crystalline  $\text{Co}_{1.5}\text{Fe}_{1.5}\text{Ge}$  (001) films were grown by molecular beam epitaxy. The structure of the films is cubic with the expected lattice constant. All the structural and magnetic characterizations clearly indicate chemical ordering consistent with the full Heusler structure. In particular, very low Gilbert damping coefficients are obtained. However, some chemical disorder involving Co atoms occupying in Y sites instead of Fe cannot be ruled out here, which would lead in accordance to our theoretical investigations to a suppression or reduction of the pseudo gap at the Fermi level. The spin-polarization of CFG(001) at  $E_F$  is observed to be positive opposed to the negative spin-polarization of FeCo(001), and, furthermore it is not 100%. The pseudo-gap for minority spin at  $E_F$  is not observed. Some minority spin DOS with  $\Delta_1$  symmetry was observed at the Fermi energy explaining the modest TMR values observed in MgO-based MTJs using CFG electrodes.

The authors thank G. Lengaigne (IJL) for patterning the magnetic tunnel junctions.

- <sup>1</sup>T. Graf, C. Felser, and S. S. P. Parkin, *Prog. Solid State Chem.* **39**, 1–50 (2011), and references therein.
- <sup>2</sup>M. Ding and S. J. Poon, *Appl. Phys. Lett.* **101**, 122408 (2012).
- <sup>3</sup>H. Lee, Y.-H. A. Wang, C. K. A. Mewes, W. H. Butler, T. Mewes, S. Maat, B. York, M. J. Carey, and J. R. Childress, *Appl. Phys. Lett.* **95**, 082502 (2009).
- <sup>4</sup>S. Maat, M. J. Carey, and J. R. Childress, *Appl. Phys. Lett.* **93**, 143505 (2008).
- <sup>5</sup>K. Özdoğan, B. Aktaş, I. Galanakis, and E. Şaşıoğlu, *J. Appl. Phys.* **101**, 073910 (2007).
- <sup>6</sup>K. R. Kumar, K. K. Bharathi, J. A. Chelvane, S. Venkatesh, G. Markandeyulu, and N. Harishkumar, *IEEE Trans. Magn.* **45**, 3997 (2009).
- <sup>7</sup>Y. K. Takahashi, A. Srinivasan, B. Varaprasad, A. Rajanikanth, N. Hase, T. M. Nakatani, S. Kasai, T. Fu-rubayashi, and K. Hono, *Appl. Phys. Lett.* **98**, 152501 (2011).
- <sup>8</sup>M. Zhu, B. D. Soe, R. D. McMichael, M. J. Carey, S. Maat, and J. R. Childress *Appl. Phys. Lett.* **98**, 072510 (2011).
- <sup>9</sup>C.-H. Lambert, A. Rajanikanth, T. Hauet, S. Mangin, E. E. Fullerton, and S. Andrieu, *Appl. Phys. Lett.* **102**, 122410 (2013).
- <sup>10</sup>F. Albertini, A. Paoluzi, L. Pareti, G. Turilli, A. Y. Ermakov, N. Mushnikov, O. Moze, and L. Calestani, *J. Magn. Magn. Mater.* **140–144**, 141 (1995).
- <sup>11</sup>G. Kresse and J. Furthmüller, *Phys. Rev. B* **54**, 11169 (1996).
- <sup>12</sup>J. P. Perdew, J. A. Chevary, S. H. Vosko, K. A. Jackson, M. R. Pederson, D. J. Singh, and C. Fiolhais, *Phys. Rev. B* **46**, 6671(1992).
- <sup>13</sup>C. Bilzer, T. Devolder, J.-V. Kim, G. Counil, C. Chappert, S. Cardoso, and P. P. Freitas, *J. Appl. Phys.* **100**, 053903 (2006).
- <sup>14</sup>T. Devolder, T. Tahmasebi, S. Eimer, T. Hauet, and S. Andrieu, *Appl. Phys. Lett.* **103**, 242410 (2013).
- <sup>15</sup>F. Bonell, T. Hauet, S. Andrieu, F. Bertran, P. Le Fèvre, L. Calmels, A. Tejada, F. Montaigne, B. Warot-Fonrose, B. Belhadji, A. Nicolaou, and A. Taleb-Ibrahimi, *Phys. Rev. Lett.* **108**, 176602 (2012).
- <sup>16</sup>K. Dumesnil and S. Andrieu, “Molecular beam epitaxy: From quantum wells to quantum dots. From research to mass production,” *Epitaxial Magnetic Layers Grown by MBE: Model Systems to Study the Physics in Nanomagnetism and Spintronic*, edited by M. Henini (Elsevier, 2012), Chap. XX.
- <sup>17</sup>L.-N. Tong, F. Matthes, M. Müller, C. M. Schneider, and C.-G. Lee, *Phys. Rev. B* **77**, 064421 (2008).